

# A Sensitivity Analysis Study of the SPITFIRE Fire Model

J L Gómez-Dans<sup>a,b,\*</sup>, A Spessa<sup>c</sup>, M Wooster<sup>a</sup>, P Lewis<sup>b</sup>

<sup>a</sup>*Department of Geography, King's College London, Strand, London, WC2R 2LS, United Kingdom*

<sup>b</sup>*Department of Geography, University College London, Pearson Building, Gower Street, WC1E 6BT, United Kingdom*

<sup>c</sup>*Department of Meteorology, University of Reading, Earley Gate, PO Box 243, Reading, RG6 6BB, United Kingdom*

---

## Abstract

*Keywords:* fire modelling, sensitivity analysis, DGVM, vegetation modelling

---

## Contents

<b>1</b>	<b>Introduction</b>	<b>2</b>
<b>2</b>	<b>Materials</b>	<b>4</b>
2.1	Model description . . . . .	4
2.2	Sensitivity analysis . . . . .	6
2.2.1	The Morris screening method . . . . .	6
2.2.2	The Sobol' SA procedure . . . . .	7
2.2.3	Assessing the robustness of the SA results . . . . .	8
2.3	Fire model drivers . . . . .	9
2.4	Site descriptions . . . . .	9
2.4.1	Boreal . . . . .	10
2.4.2	Savannas . . . . .	10
2.4.3	Temperate . . . . .	10
2.4.4	Tropical . . . . .	11
<b>3</b>	<b>Results</b>	<b>11</b>
3.1	Individual model components . . . . .	11
3.1.1	Potential ignitions . . . . .	11
3.1.2	Fuel moisture dynamics . . . . .	12
3.1.3	Rate of spread . . . . .	12
3.2	Sensitivity analysis per biome . . . . .	13
3.2.1	Boreal forests . . . . .	13
3.2.2	Savannahs . . . . .	14
3.2.3	Temperate regions . . . . .	15
3.2.4	Tropical rainforest . . . . .	15
<b>4</b>	<b>Discussion</b>	<b>16</b>
<b>5</b>	<b>Conclusions</b>	<b>18</b>

---

\*Corresponding author

*Email addresses:* [j.gomez-dans@geog.ucl.ac.uk](mailto:j.gomez-dans@geog.ucl.ac.uk) (J L Gómez-Dans),  
[a.spessa@reading.ac.uk](mailto:a.spessa@reading.ac.uk) (A Spessa), [m.wooster@kcl.ac.uk](mailto:m.wooster@kcl.ac.uk) (M Wooster),  
[plewis@geog.ucl.ac.uk](mailto:plewis@geog.ucl.ac.uk) (P Lewis)

## 1. Introduction

Fire is the main source of disturbance to vegetation, present in all biomes and continents (Van der Werf et al., 2006). As such, the description of fire and its effects on vegetation is an important part of quantifying fluxes from the land sink to the atmosphere (Giglio et al., 2005; Randerson et al., 2005). Fire is a complex phenomenon, regulated by climate, vegetation and human activity, in turn impacting vegetation productivity, succession and (Bergeron et al., 2004; Goldammer and Furyaev, 1996; Cochrane, 2003; Whelan, 1995). Fire controls are different in different ecosystems: in the boreal region, temperature controls fire occurrence (Flannigan et al., 2005), and limits the length of the fire season. In semi-arid, savannas and mediterranean ecosystems, typically exhibiting seasonal or inter-annual rainfall patterns, it is fuel availability that controls fires (Randerson et al., 2005; Archibald et al., 2009). In the tropics, precipitation controls fires, either by depressing its occurrence in moist rainforests (Cochrane, 2003), or by promoting biomass accumulation during the wet season in tropical savannas. The variability of burned area in these ecosystems appears related to El Niño -Southern-Oscillation occurrence (Harris et al., 2008; Randerson et al., 2005; Kitzberger et al., 2001; van der Werf et al., 2008).

Analyses of fire activity patterns and the factors driving these patterns, are predominantly based on Earth Observation (EO) data [REFS!!]. High quality EO data has only emerged within the last decade or so, and hence cannot be used to assess fire activity that occurs over multidecadal timescales. Also, EO data cannot be used to predict fire activity and its effects in the future. Models that make predictions outside the contemporary satellite data record are clearly necessary. We stress the necessity of these models being thoroughly validated as well as providing estimates of uncertainties in modelled magnitudes.

Prognostic fire models, embedded in dynamic global vegetation models (DGVMs) can in principle simulate the effects of changes in climate and vegetation dynamics as a bidirectional feedback with the embedded fire model. This capability allows us to investigate how fire and fire-related emissions might change with changing climate conditions and vegetation dynamics. There have been several attempts to simulate fire as an interactive component of DVMS (Lenihan et al., 1998; Thonicke et al., 2001; Venevsky et al., 2002; Arora and Boer, 2005; Lehsten et al., 2008). Such models are primarily designed to incorporate the role of fire as a disturbance factor for vegetation dynamics and to account for corresponding fluxes in the global carbon cycle. Trace gas and aerosol emissions can also be derived within these models via the use of emissions factors, that map combusted biomass into amounts of emitted species (Andreae and Merlet, 2001).

The SPITFIRE (SPread of and InTensity of FIRE) fire model has been designed to overcome some limitations of previous fire models set within DGVM frameworks, while being flexible enough to allow both global and regional simulations using only minimal input data requirements (Thonicke et al., 2010). SPITFIRE was originally developed as an embedded module within the LPJ DGVM framework and is a

44 successor to the RegFIRM fire model (Venevsky et al., 2002). RegFIRM explicitly  
45 simulates processes of climatic fire danger and lightning and human caused ignitions.  
46 SPITFIRE builds on this treatment with a more complete representation of ignitions  
47 and fire spread (if conditions are conducive to fires spreading), and comprises new  
48 process-based submodels of fire intensity and the risk of vegetation dying from  
49 either crown scorch or cambial death (the two most important causes of post-fire  
50 mortality), as well as emissions of trace gases and aerosols from biomass burning.  
51 The basic premise behind SPITFIRE is that one needs three precursors to fire  
52 occurrence: an ignition source (lightning or human-related), a sufficient amount of  
53 fuel, and a fuel bed that is dry enough (Pyne et al., 1996). In summary, the model  
54 tries to account for

- 55 • ignition sources (both human and lightning strikes),
- 56 • fuel types,
- 57 • fuel susceptibility to fire through modelling of fuel moisture dynamics,
- 58 • fire spread dynamics,
- 59 • crown scorching versus ground fires,
- 60 • modelling of fire-induced plant mortality.

61 This ambitious choice of processes adds a considerable degree of complexity to  
62 the model. This complexity manifests itself in a large set of parameters that control  
63 the different sub-models. However, there is a paucity of ground data in the literature  
64 with which to parametrise the model, with the added complication that these studies  
65 are usually biome, location or scale dependent. Due to the strong non-linearities and  
66 strong coupling between different sub-models, effects of individual parameters in the  
67 typical model outputs considered as model diagnostic (burned area, number of fires,  
68 emissions, etc.) are often difficult to isolate. The implication is that it is difficult to  
69 see what parameters can be constrained by what diagnostic observations. For global  
70 applications, users have to rely on the availability of a handful of imperfect datasets  
71 describing burned area or combusted biomass, typically derived from EO platforms,  
72 and perform an inverse modelling exercise [REF], in which the model parameters are  
73 treated like variables and tweaked so as to fit the observations within their margin  
74 of error. The limitation of a few noisy products available for inverse modelling  
75 studies limits the number of parameters that can be effectively constrained. In  
76 some circumstances, parameters may need to lose part of its physical meaning and  
77 become “effective”. It is thus important to concentrate on parameters that can  
78 be effectively constrained by the available observations, or in other words, on a  
79 reduced set of key parameters that demonstrably display the strongest contribution  
80 to model output in comparison to a calibration standard.

81 A crucial step towards defining a set of key parameters for any model is to carry  
82 out a comprehensive sensitivity analysis (SA) exercise, where the impact of model  
83 parameters in model output is assessed and parameters are ranked by importance

84 (Saltelli et al., 2004). This paper performs a comprehensive SA of the SPITFIRE  
 85 model, focussing on parameters influencing the simulation of burnt area and a  
 86 sample of sites covering a range of biomes. We seek to identify which parameters and  
 87 parameter combinations in the fire model, when perturbed cause the biggest changes  
 88 to burnt area. We use an off-line version of SPITFIRE, in which climate and biomass  
 89 inputs to the fire model are prescribed by daily meteorology and monthly biomass  
 90 data based on CASA/GFED (Van der Werf et al., 2006) simulations. Vegetation  
 91 inputs were prescribed because the focus is in the behaviour of the fire model, and  
 92 the feedback between fire and vegetation only complicates this endeavour. The  
 93 results of the SA work are used to assess the importance of different parameters  
 94 in the fire model across different biomes, and what this means for improved fire  
 95 prediction.

96 We propose to carry out such work in this paper, using an off-line version of the  
 97 SPITFIRE model. This is done by feeding the model meteorological and vegeta-  
 98 tion inputs and then running the SPITFIRE model for each day in the year. The  
 99 vegetation is calculated using the GFED/CASA model, a vegetation model that is  
 100 driven by monthly meteorological inputs and EO data. Typical climatic patterns,  
 101 including inter-annual variability, as well as variation of fuel loads and types, need  
 102 to be taken into account to assess sensitivity of the fire model to its drivers. Further,  
 103 we hypothesise that for different biomes, different sets of parameters are likely to  
 104 be of importance.

## 105 2. Materials

### 106 2.1. Model description

107 [Figure 1 about here.]

108 The SPITFIRE fire model is described in depth in (Thonicke et al., 2010), but  
 109 this Section provides a brief description of how the model calculates burned area.  
 110 A diagram is shown in Fig. 1. SPITFIRE is fed fuels in terms of 1-hr, 10-hr,  
 111 100-hr and 10000-hr fuel loads per plant functional type (PFT) from a dynamic  
 112 global vegetation model (DGVM). Other inputs relate to daily series of phenol-  
 113 ogy, soil moisture, wind speed, precipitation, minimum, maximum and mean daily  
 114 temperatures. Above and below ground litter pools are also required. SPITFIRE  
 115 calculates the number of potential ignitions due to human activity (function of  
 116 population density and observation-based estimates of the spatial distribution of  
 117 human-caused ignitions across model cells) and lightning strikes (from an observed  
 118 lightning climatology dataset). The Nesterov Index ( $NI$ ), defined as

$$NI = \sum T_{max}(d) \cdot (T_{max}(d) - T_{dew}(d)), \quad (1)$$

119 where  $T_{max}$  and  $T_{dew}$  are the daily maximum and dew-point temperature. In Eq. 1,  
 120 the summation is an accumulation that is reset when precipitation for a given day  
 121 is greater than 3mm. The Nesterov Index is used as a basis to calculate the

122 moisture content of the different fuel pools:

$$\omega_o = \exp \left\{ - \left[ \sum_{i=1}^3 \alpha_i \cdot \frac{w_{oi}}{w_o} \right] \cdot NI \right\}, \quad (2)$$

123 where  $w_{oi}$  is the amount of fuel in the 1-, 10- and 100-hr fuel classes,  $w_o$  is the total  
 124 fuel, and  $\alpha_i$  is a constant that controls the scaling of  $NI$  weighted by the relative  
 125 abundance of each fuel class. For each fuel class,  $\alpha$  is defined as the value of  $\alpha_{1hr}$   
 126 divided by the ratio of surface-area to volume value of the 1-hr fuel class to the fuel  
 127 class in question:

$$\alpha_i = \alpha_{1hr} \cdot \frac{\sigma_i}{\sigma_{1hr}}. \quad (3)$$

128 An additional and important use of  $NI$  is in defining a (normalised) fire danger  
 129 index (FDI), that is zero if  $\omega_o$  is higher than the moisture of extinction,  $m_e$ , or if  
 130 no fuel is available. Otherwise, it is calculated as  $1 - \frac{\omega_o}{m_e}$ , explicitly

$$FDI = \max \left\{ 0, \left[ 1 - \frac{1}{m_e} \cdot \exp \left\{ - \left[ \sum_{i=1}^3 \alpha_i \cdot \frac{w_{oi}}{w_o} \right] \cdot NI \right\} \right] \right\}. \quad (4)$$

131 The fuel types and loads present in the simulation unit are used to specify a  
 132 number of variables related to fuel structure. Combined with the moisture content  
 133 and environmental variables, Rothermel's fire spread equations (Rothermel, 1972)  
 134 are used to calculate rate of spread ( $RoS$ ), the speed at which the fire front advances.  
 135 This quantity is given by

$$RoS = \frac{I_R \cdot \xi (1 + \Phi_w)}{\rho \cdot \epsilon \cdot Q_{ig}}. \quad (5)$$

136 In Eq. 5,  $I_R$  is the reaction intensity (the energy release per unit area of the fire  
 137 front),  $\xi$  is the propagating flux ration (the proportion of the reaction intensity that is  
 138 used to heat up adjacent fuel particles to ignition), and  $\Phi_w$  is a scalar that accounts  
 139 for the effect of wind in increasing the value of  $\xi$ . The denominator is made up of the  
 140 product of the fuel bulk density,  $\rho$ , assigned per PFT and weighted by fuel class.  
 141  $\epsilon$  is the effective heating number, and expresses the proportion of a fuel particle  
 142 that is heated to ignition temperature at the time flaming combustion starts.  $Q_{ig}$   
 143 is the heat of pre-ignition, or the amount of heat required to ignite a mass of fuel.  
 144 Clearly, the numerator of Eq. 5 accounts for fire spread, while the denominator  
 145 can be seen as a dampening of spread due to fuel geometry, moisture content and  
 146 composition of the fuel. Due to the need of using daily meteorological drivers,  
 147 this estimate of  $RoS$  is necessarily an approximation to the steady state, and it  
 148 is also assumed identical for all fires spreading in the region (usually defined as a  
 149 gridcell with constant climatic drivers. Typical sizes range from tenths to one or  
 150 two degrees). The area burned by this 'average fire' is calculated assuming fires are  
 151 elliptical, with the product of  $RoS$  and fire duration (calculated as a function of a  
 152 maximum fire duration and the  $FDI$ ) determining the size major axis of the ellipse,  
 153 and the length-to-breadth ratio  $LB$  (a function of wind speed, and calculated as per  
 154 (Canadian Forestry Service, 1992)) determining the minor axis. This 'average fire

155 size’ is multiplied by the number of potential ignitions to obtain realised ignitions.  
 156 The intensity of the fire at the flaming front,  $FI$  is calculated as per (Byram and  
 157 Davis, 1959):

$$FI = H \cdot RoS \cdot W_c, \quad (6)$$

158 where  $H$  is the heat content of the fuel,  $RoS$  is the rate of spread, and  $W_c$  is the total  
 159 combusted fuel in the 1-hr, 10-hr and 100-hr fuel classes. In turn, combusted fuel is  
 160 a function of fuel moisture, and is calculated using the empirical relationships based  
 161 on (Peterson and Ryan, 1986).  $FI$  is used as a condition to decide whether realised  
 162 fires spread: fires will only spread if  $FI \geq 50kWm^{-1}$  (after Pyne et al. (1996)).  
 163  $I_{surface}$  is used, in addition to calculate residence time (a function of Rothermel’s  
 164 reaction intensity) and some PFT-specific parameters, to calculate the impact of  
 165 fire on vegetation, as well as other fire properties (flame height, crown scorching,  
 166 ground fires, ...).

## 167 2.2. Sensitivity analysis

168 Sensitivity analysis (SA) aims to provide an assessment of the influence of a  
 169 parameter or factors on model output (Saltelli et al., 2004). In general, the influence  
 170 of parameters in the output is examined by sweeping the value of these parameters  
 171 over their range of uncertainty, running the model forward, and examining the  
 172 output. Typical approaches to analysing the output include analysis of variance or  
 173 regression-based methods (Campolongo and Saltelli, 1997; Archer et al., 1997). The  
 174 former require numerous runs, and result in an computationally intractable problem.  
 175 The latter are not ideally suited to complex non-linear models as SPITFIRE. A  
 176 proxy for the variance-based methods is the screening method of Morris (Morris,  
 177 1991; Campolongo et al., 2007), which requires a relatively modest number of model  
 178 executions to rank factors. The Morris technique has been successfully applied to  
 179 assess the sensitivity of crop models (Confalonieri et al., 2009, 2010), and a snow  
 180 cover dynamics model (Thorsen et al., 2010).

181 In this study, we use the Morris technique for complete model runs, as using a  
 182 variance method would result in an unmanageable computational cost. For exam-  
 183 ining individual sub-processes or modules in SPITFIRE, we revert to the variance-  
 184 based method (since modules contain far fewer parameters than the whole model).  
 185 The results of the Morris method are found to be comparable to the variance meth-  
 186 ods in (Confalonieri et al., 2010) and (Campolongo and Saltelli, 1997).

### 187 2.2.1. The Morris screening method

188 The Morris screening method is based on the calculation of the so-called ‘ele-  
 189 mentary effects’ of each model input factor. The elementary effect is defined as

$$R_i(x_i, \dots, x_N, \Delta) = \frac{M(x_1, \dots, x_{i-1}, x_i + \Delta, \dots, x_N) - M(x_1, \dots, x_N)}{\Delta}. \quad (7)$$

190 In Eq. 7, the model output is  $M(\underline{x})$ , where  $\underline{x}$  is the  $N$ -dimensional input vector of  
 191 model parameters.  $\Delta$  is a value related to a discretisation of parameter space into  
 192  $p$  levels, and is a value between  $1/(p-1)$  and  $1-1/(p-1)$ .

193 The Morris method calculates the elementary effects of each parameter by sam-  
 194 pling random trajectories over the (discretised) parameter space, where each point  
 195 in a trajectory differs from the previous one in  $\pm\Delta$  for only one factor, the rest being  
 196 kept identical (this is called “one-at-a-time” sampling). Once parameter space has  
 197 been traversed by the random trajectories and elementary effects for each factor  
 198 have been calculated, the mean  $\mu$  and standard deviation,  $\sigma$  are calculated.  $\mu$  is  
 199 related to the influence of each parameter in the output, whereas  $\sigma$  accounts for the  
 200 combined effect of the parameter in question with other parameters, the so-called  
 201 higher order effects. In (Campolongo et al., 2007), the use of the absolute value  
 202 of  $\mu$ , termed  $\mu^*$  is recommended, as it avoids ambiguity when ranking parameters.  
 203 A further enhancement is in the way trajectories along parameter space are calcu-  
 204 lated. (Campolongo et al., 2007) also introduces a way of generating trajectories  
 205 that maximise parameter space filling.

206 To illustrate the analysis procedure consider Fig. 2, depicting some hypothetical  
 207 results of a Morris analysis applied to a model with 5 parameters or factors:  $A$ ,  $B$ ,  
 208  $C$ ,  $D$  and  $E$ . Parameter  $A$  is characterised by a high value of  $\mu^*$  and a low value of  
 209  $\sigma$ , suggesting that this parameter has a strong direct effect on the output, but does  
 210 not interact very much with other parameters. Parameters  $B$  and  $C$  have a similar  
 211 effect on the output, but the higher  $\sigma$  values indicate that the indirect or higher  
 212 order effects are much larger.  $D$  has a small effect on the output, but is strongly  
 213 coupled with other parameters, while the effect of  $E$  is negligible. This example  
 214 would suggest that  $A$ ,  $B$  and  $C$  have an important effect on the output (high values  
 215 of  $\mu^*$ ), whereas  $D$  and  $E$  have only a very marginal effect. Additionally,  $B$  and  $C$   
 216 also show important higher order interactions or indirect effects.

217 [Figure 2 about here.]

### 218 2.2.2. The Sobol’ SA procedure

219 The Sobol’ method has much in common with ANOVA methodologies (Helton  
 220 et al., 2006). It aims to partition the total variance of the model into a weighted  
 221 summation of the individual effects of each factor:

$$222 \quad V(y) = \sum_{i=1}^N D_i + \sum_{i \leq j < \leq N}^N D_{i,j} + \dots + \sum_{i \leq \dots N}^N D_{i,\dots,N}, \quad (8)$$

223 where  $D_i$  is the first order (direct) effect for each factor  $x_i$  and  $D_{i,j}$  is the effect of  
 224 the interaction between parameters  $x_i$ . Two indices are defined to account for first  
 and higher order sensitivities:

$$225 \quad S_i = \frac{D_i}{V(y)} \quad (9)$$

$$226 \quad S_{Ti} = \frac{V(y) - D_{\sim i}}{V(y)} \quad (10)$$

In Eq. 10,  $D_{\sim i}$  is the sum of all variance terms that do not include term  $i$ .  $S_i$   
 is then the direct impact of factor  $i$  on the model output, the first order effect.

227  $S_{Ti}$  is the combined effect, or higher order effect of the factor  $i$  on the output, the  
 228 term that quantifies the effect of the interaction between parameter  $i$  and the other  
 229 parameters have on the output. Both of these parameters are bounded between zero  
 230 and one, with factors characterised by values close to unity having an important  
 231 effect on the output.

232 As pointed at the beginning of this Section, variance-based decompositions are  
 233 extremely useful, but computationally costly. The often-used Sobol' method re-  
 234 quires  $nS \cdot (2N + 2)$  model evaluations, where  $nS$  is the number of samples required  
 235 to estimate the variance. In Saltelli (2002), an extension that calculates the Sobol'  
 236 indices for both first-order and total indices at the same time (altogether  $2N$  in-  
 237 dices), at a total cost of  $(N + 2) \cdot nS$  model evaluations.

### 238 2.2.3. Assessing the robustness of the SA results

239 We chose sites that are representative of the range of biomes affected by fire.  
 240 In order to explore the uncertainty in other factors not directly related to the fire  
 241 model, such as inter-annual weather variability, the effect of uncertainty of fuel  
 242 load estimates, and of demographic parameters affecting human-induced ignitions,  
 243 replicates of the SA exercise were carried out for each site. These replicates comprise  
 244 a selection of grid cells around a central site gridcell, that aim to capture variability  
 245 at the site. Since the SA results are different for each replicate, we investigated the  
 246 consistency of the results. As in Confalonieri et al. (2009), we choose to use the top  
 247 down concordance coefficient (TDCC) (Helton et al., 2006), a way of estimating the  
 248 concordance of the rank ordering of factors in each replicate. The TDCC enhances  
 249 the contribution of important (highly ranked) parameters, while depressing the  
 250 effect of irrelevant parameters. Its calculation is straightforward: start by defining  
 251  $SM_{ij}$ , the sensitivity measure of parameter  $i$ , with  $j = 1, \dots, n_R$  being the replicate  
 252 number.  $r(SM_{ij})$  being the rank order associated with parameter  $i$ , replicate  $j$  (1  
 253 for the most important parameter, 2 for the second most important, etc.) Next,  
 254 calculate the Savage scores as

$$ss(SM_{ij}) = \sum_{i=r(SM_{ij})}^N i^{-1}. \quad (11)$$

255 The Savage scores are then used to calculate the TDCC (Helton et al., 2006) as

$$TDCC = \frac{\sum_{i=1}^N \left[ \sum_{j=1}^{n_R} ss(SM_{ij}) \right]^2 - n_R^2 \cdot N}{n_R^2 \cdot \left[ N - \sum_{i=1}^N i^{-1} \right]}. \quad (12)$$

256 The TDCC provides an indication of how similar the rank ordering is between  
 257 different replicates, and gives an idea of the consistency of the sensitivity analysis  
 258 for a given biome. High values (close to unity) imply that the results are similar,  
 259 whereas low values indicate that the results are heterogeneous. Note that the latter  
 260 situation is not necessarily an indication of poor SA performance, as it can arise due  
 261 to adjacent grid cells being different in terms of demography, climate, fire history,  
 262 etc.

263 *2.3. Fire model drivers*

264 A number of drivers are required to run SPITFIRE. These are:

- 265 1. daily meteorological data (precipitation, dew point, wind speed, minimum,  
266 maximum and mean temperatures) and monthly lightning climatology,
- 267 2. phenology,
- 268 3. top level soil moisture,
- 269 4. PFTs present in the grid cell (as well as projected fractional coverage),
- 270 5. fuel loads per PFT and fuel class,
- 271 6. population density.

272 The daily meteorological drivers and top layer soil moisture were obtained from  
273 the NCEP Reanalysis dataset (Kalnay et al., 1996), and interpolated to 0.5 degrees.  
274 The lightning flash monthly climatology is derived from gridded satellite lightning  
275 data produced by the NASA LIS/OTD Science Team (Principal Investigator, Dr.  
276 Hugh J. Christian, NASA / Marshall Space Flight Center). The PFTs present  
277 in each grid cell were derived from the MODIS land cover product (MCD12Q1).  
278 Demographic information is derived from a resampled version of the HYDE3 dataset  
279 (Goldewijk, 2005). Phenology is only relevant to grasses in SPITFIRE, so it was  
280 derived from a scaled trajectory of the monthly MODIS NDVI fitted with a spline  
281 polynomial to obtain a daily phenology estimate in the range [0, 1].

282 Fuel loads were simulated with CASA model (Potter et al., 1993; van der Werf  
283 et al., 2004; Van der Werf et al., 2003; van der Werf et al., 2010) driven by MODIS  
284 monthly NDVI data from 2000 to 2005. Monthly NCEP Reanalysis data were used  
285 as inputs for CASA. Burned area data from the GFED dataset were used (Giglio  
286 et al., 2010), but for the purpose of this work, monthly fuel loads were calculated  
287 without fire disturbance. The model output with observed fire disturbance is used  
288 as the starting state for each annual run. The maximum fuel load per year was fed  
289 into SPITFIRE. The different litter pools in CASA were associated with different  
290 fuel classes, and divided among all the present PFTs weighted by percentage area  
291 covered. The mapping from CASA/GFED pools to SPITFIRE fuel classes was as  
292 follows: The 1-hr fuel class comprised the tree and grass leaf mass, as well as the  
293 grass fine litter contribution. The 10-hr fuel class was made up of fine tree litter.  
294 The 100-hr class had the tree coarse debris pool and the 1000-hr class included the  
295 tree trunks.

296 *2.4. Site descriptions*

297 Fire is a function of ignitions, climate and vegetation, as well as having a condi-  
298 tioning feedback on them (Pyne et al., 1996). Some of these factors can be broadly  
299 studied at the biome level (for example, savannas tend to be dominated by grasses  
300 while tropical rainforests are dominated by trees), but nonetheless very important  
301 to consider how the fire model behaves for the same biome under different weather  
302 forcings, or by exploring the effect of heterogeneous landcover or demographics.  
303 For example, consider a boreal site where one year is characterised by drought,

304 and hence high fire activity, which results in a removal of most of the vegetation.  
305 Surrounding sites escape fires during this year even though they possess a suffi-  
306 cient amount of fuel either because of insufficient ignitions and/or the drought was  
307 localised in its effect. In subsequent drought years we would expect the site in  
308 question to experience little fire activity because most of its vegetation has been  
309 removed and vegetation regrowth in high latitudes is comparativeky low. However,  
310 this will not apply to the adjacent sites, which may well burn if a confluence of  
311 drought conditions and ignitions occur in the future. This example illustrates the  
312 importance of having replicate sites to take into account within-biome variability.

313 Several sites were chosen to be representative of the boreal, savanna, temperate  
314 and tropical regions. For each site, a central grid cell was chosen. A range of 25  
315 cells are chosen randomly within a radius of 2 degrees around the central grid cell.  
316 In the following sections, we describe the sites grouped by biome.

317 [Table 1 about here.]

318 [Figure 3 about here.]

#### 319 *2.4.1. Boreal*

320 [Figure 4 about here.]

321 The sites in the Boreal region are characterised by cold climates, with snow  
322 during the winter, and precipitation during summer. The main PFT is needleleaved  
323 evergreen trees, which results in fuel distributions with similar contributions to the  
324 1-hr, 10-hr and 100-hr fuel classes. In combination with the low temperatures,  
325 the fuel loads result in the *FDI* rising slowly after a rain event (see Fig. 4), with  
326 fuel moisture being high unless a large dry spell takes place. The Canada site is  
327 unpopulated, the other sites do however have significant population densities. This  
328 means that in the Canada site, the only ignition sources will be lightning strikes.

#### 329 *2.4.2. Savannas*

330 [Figure 5 about here.]

331 The savanna sites have clear dry/wet season dynamics, with high temperatures.  
332 The main PFTs are grasses, resulting in little or no fuel loads in the 10-hr or 100-hr  
333 classes. As fuel accumulation is controlled by precipitation during the rainy season,  
334 inter-annual fuel availability is typically dependent on precipitation. Additionally,  
335 since fires are frequent, there is not much chance of multi-annual litter accumulation,  
336 so that fuel loads are in general low for all the sites considered [REFERENCE].  
337 The *FDI* is practically unity throughout the dry season (Fig. 5), resulting in no  
338 impediment to fires taking place during this period.

#### 339 *2.4.3. Temperate*

340 [Figure 6 about here.]

341 The temperate region sites are quite heterogenous, both in terms of vegetation  
 342 and in terms of climate. While the California site is fairly indistinguishable from  
 343 other savanna sites (for example, compare the *FDI* plots for California, Fig. 6(b),  
 344 and Northern Australia, Fig. 5(d)), the Iberia site is characterised by having a few  
 345 dry spells in the summer, and a heterogenous mixture of fuel types. The Argentina  
 346 site is mainly covered in grasses, and has a number of rainfall events during the  
 347 austral summer, but high temperatures result in fast drying out of fuels.

#### 348 2.4.4. Tropical

349 [Figure 7 about here.]

350 The tropical region sites are typical rainforest sites in the Amazon and Borneo.  
 351 They are characterised by high fuel loads, high relative humidity, high precipita-  
 352 tion and high temperatures. In general, these sites are not fire-prone due to the  
 353 continuous precipitation and high fuel moisture (Cochrane, 2003), as is obvious for  
 354 the temporal plots of *FDI* shown in Fig. 7. There can, however, be years where  
 355 drought conditions result in increased flammability, in particular in the Amazonas  
 356 site, as there is a small proportion of grid cells with fairly high concentration of C4  
 357 grasses (up to 23% for some cells). This is not the case in Borneo, where all the  
 358 gridcells are almost exclusively covered with tropical evergreen trees. We note that  
 359 in (Thonicke et al., 2010), SPITFIRE substantially underestimates burned area for  
 360 the tropical region.

### 361 3. Results

#### 362 3.1. Individual model components

363 In the first instance, it is instructive to examine how parameters affect individual  
 364 model components of the model, rather the whole model itself. In the case of  
 365 SPITFIRE, we focus on the three main modules governing simulated area burnt:  
 366 ignitions, fuel moisture dynamics and rate of spread.

##### 367 3.1.1. Potential ignitions

368 Ignitions are modelled as the sum of lightning strikes ignitions and human igni-  
 369 tions. The former are derived by scaling an observed lightning flash climatology  
 370 derived from satellite observations. A constant proportion of these flashes are as-  
 371 sumed to be cloud-to-ground lightning strikes, and are thus a source of potential  
 372 ignitions. Human ignitions sources, on the other hand, are modelled on the basis  
 373 that as humans move into an area, fire is used to manage the land, clear forests,  
 374 etc. After population grows, the combined effect of landscape fragmentation, ex-  
 375 tinction efforts, as well as the move towards less fire-intensive economic activities,  
 376 results in a drop in the observed fire activity (Cochrane et al., 1999). In SPITFIRE,  
 377 human ignitions are then a scaling of the population density,  $P_D$ , through a non-  
 378 linear function, that is then converted to potential human ignitions using an extra  
 379 parameter:

$$n_{h,ig} = P_D \cdot 30 \cdot \exp\left[-0.5\sqrt{P_D}\right] \cdot \frac{a_{Nd}}{100} \quad (13)$$

380 The exponential term in Eq. 13 has a peak for values of  $P_D$  of  $16km^{-2}$ .

381 In both lightning stike and human ignitions, the number of ignitions is directly  
382 proportional to the proportion of observed flashes that are deemed to be cloud-to-  
383 ground ones, and to the parameter that expresses the likelihood of humans igniting  
384 fires ( $a_{Nd}$ ).  $a_{Nd}$  has units of ignitions per individual per fire season day (Thonicke  
385 et al., 2010). Clearly, these two parameters directly modulate the total number of  
386 potential ignitions, which in turn governs overall burned area.

### 387 3.1.2. Fuel moisture dynamics

388 In SPITFIRE, fuel moisture dynamics is governed by climate through the calcu-  
389 lation of the Nesterov Index, fuel loads per fuel class and the moisture of extinction  
390 of different PFTs. The relative moisture content of all fuels is calculated from the  
391 NI, scaled by a weighted average of the contribution of each fuel type and a param-  
392 eter that relates to the surface to area volume of the fuel class, as shown in Eq. 2.  
393 The rationale behind Eqns. 2 and 3 is to allow 1-hr fuels such as grasses, charac-  
394 terised by high SAV values to dry faster than low SAV 10-hr or 100-hr fuels (e.g.,  
395 branches). In addition to this, if live grasses are present in the simulation unit, the  
396 1-hr fuel class moisture content is modified by the livegrass moisture content. The  
397 latter is a function of top layer soil moisture (Thonicke et al., 2010).

398 The abundance of one or more types of fuels, coupled with the climatic history  
399 that defines the NI, are the major drivers of fuel moisture dynamics. In this respect,  
400 it is likely that different biomes will react very differently to factors controlling fuel  
401 moisture. For example, savannas tend to be characterised by a long dry season,  
402 with consistently high values of NI; the fuel load tends to be largely dominated  
403 grass, resulting in preponderance of dry 1hr fuels. In the boreal region, short dry  
404 spells and a mixture of the fuel types will make for a different impact of factors in  
405 fuel moisture. In the tropics, long dry seasons are needed to dry out the fuels. As  
406 such, any conclusion on the effect of model parameters on moisture dynamics will  
407 necessarily need to be biome and climate specific. Although in general, it can be  
408 said that parametrisations that result in fuels drying out faster will tend to increase  
409 burned area via increased  $RoS$  (see Eq. 5).

### 410 3.1.3. Rate of spread

411 [Table 2 about here.]

412 [Table 3 about here.]

413 Rate of spread is calculated using Rothermel’s equations (Rothermel, 1972; Pyne  
414 et al., 1996). In this Section, we carry out a sensitivity analysis on the different  
415 parameters that play a role in controlling rate of spread. We use the Sobol’ method,  
416 and report the direct  $S_i$  and total effects  $S_{Ti}$  in Table 2. While the direct effects  
417 of individual parameters are all negligible, the combined effects of the fuel bulk  
418 density, the fuel moisture content, the surface-to-area volume and wind speed all  
419 are very significant.

420 It is interesting to consider a typical situation which appears often in savannas  
421 during the dry season. Firstly, we note that these sites are largely grassland sites  
422 (see Table 1). The FBD for these sites is then identical to that of C3 or C4 grasses,  
423 as there are no trees. During the dry season, the lack of rain events results in  
424 a long period where  $FDI$  is unity. Even if rain events occur, the relatively high  
425 temperatures result in very localised drops in  $FDI$ , which are of little interest here.  
426 This is evident in the plots shown in Fig. 5). In this particular situation,  $RoS$  is  
427 controlled by SAV and windspeed. Additionally, windspeed over the dry season for  
428 the savanna sites appears stationary in the NCEP dataset, so that ultimately, in  
429 these situations, SAV is the dominant factor controlling  $RoS$ . We have investigated  
430 this arguments by repeating the sensitivity analyses introduced in the previous  
431 paragraph, but only for values of fuel moisture content between 0 and 0.1. The  
432 results in Table 3 show that this is the case, even considering that  $\rho$  is given plenty  
433 of freedom to vary.

434 The two analyses presented in this Section suggest that rate of spread is largely  
435 controlled by FBD and SAV when fuels are dry. Wind speed is also important  
436 factor. A practical application of the SA work to a typical savanna environment  
437 shows that SAV controls rate of spread dynamics in typical dry season scenarios.

### 438 3.2. Sensitivity analysis per biome

439 [Table 4 about here.]

440 The parameters and parameter ranges used in the biome sensitivity analysis are  
441 presented in Table 4.

#### 442 3.2.1. Boreal forests

443 [Figure 8 about here.]

444 The chosen sites, spread over the boreal regions of Eurasia and North America,  
445 show relatively large amounts of fuel, a consequence of the predominance of needle  
446 leafed evergreen trees. The contribution of trees to different fuel classes results in  
447 important share of fuels being in the 10 or 100-hr classes, although due to litter  
448 accumulation, the 1hr fuel class also has an important role. In fact, it is the con-  
449 tribution of this latter class that enhances rate of spread through a lowering of the  
450 combined fuel bulk density and an increase of total surface area to volume ratios.  
451 Fuel bulk density is inversely proportional to rate of spread (Eq. 5). Surface area  
452 to volume ratios play an important role in the definition of the moisture content of  
453 fuels (higher values, associated with 1hr fuels, result in faster drying of fuels, and  
454 hence, in an enhancement of rate of spread).

455 In the Boreal region, dry spells need to be sufficiently long in order to dry fuels  
456 out, due to the low temperatures (see Fig. 4). If this dry period exists, and ignitions  
457 occur, then fires will spread as there is in general no shortage of fuel. The relevance  
458 of this observation is that the main controls on burned area for this area are related  
459 to fuel drying dynamics ( $\alpha$ ,  $\sigma_{1hr}$ , etc.) and ignitions. We hypothesise that this  
460 will happen in sites that have a sufficiently long dry spell to allow for fuel drying,

461 such as Canada, Siberia2 and (to a lesser extent) Alaska sites (see Figs.4(c), 4(d)  
462 and 4(a), respectively). Siberia (Fig. 4(b)), on the other hand, has abundant rain  
463 during the summer, resulting in consistently low fire danger index values. Fuels will  
464 have very little chance of drying under these conditions. For the Siberia site, we  
465 expect that only factors affecting ignitions and fire duration, as they are a direct  
466 multiplier of burned area.

467 The results from the sensitivity analysis (see Fig. 8) consistently show the  
468 important interplay of factors directly controlling the simulated daily mean fire size  
469 (such as  $\tau$ ) and fuel moisture ( $\alpha$ , the moisture of extinction values, and the SAV).  
470 The number of ignitions plays no role in the largely unpopulated Canadian site, but  
471 it does play a role in the other sites, although the relatively low population density  
472 relegates the contribution of human ignitions to a second-order effect.

473 To control fire in the higher latitudes, the parameters need to enhance the pe-  
474 riods conducive to fires, either by lowering the moisture of extinction or by drying  
475 out the fine fuels. Additionally, making fires last longer is another direct impact in  
476 the daily mean burned area that is directly transferred to the annual burned area.

477 In terms of repeatability of the results, the Canada and Siberia sites have re-  
478 latively high values of *TDCC*, whereas the Alaska and Siberia2 sites have lower  
479 values. Interannual variability of climate in the Siberia2 site is important in the ex-  
480 amined period, whereas both gridcell heterogeneity and interannual variability are  
481 important in the Alaska site. The other two sites are more homogenous in terms  
482 of vegetation and population dynamics, and have a more stable climatology during  
483 the study period, resulting in more coherent factor rank orderings. Note that all  
484 the higher ranking factors show an important contribution of higher order effects,  
485 suggesting an interplay of factors, evident in particular when several factors that  
486 control fuel moisture combine to make the fuels more or less moist.

### 487 3.2.2. *Savannahs*

488 [Figure 9 about here.]

489 Savannahs are fire prone biomes (Van Wilgen and Scholes, 1997). Climate on  
490 the chosen sites is characterised by a relatively large dry season that coupled with  
491 fairly high temperatures results in a long spell of very dry fuels (see Fig. 5, where  
492 the dry season is consistently obvious). During this period, it is the availability of  
493 fuel (limited either by wet season precipitation, directly related to fuel accumulation  
494 across these biomes or fire history (Van Wilgen and Scholes, 1997; Archibald et al.,  
495 2009)) and sources of ignition that control fire spread. The fact that the dry season  
496 is long means that vegetation will have a chance to dry out. Typically, grasses  
497 dry out quickly, so over the dry season, the only inhibiting factors affecting fires  
498 are ignitions, fuel and maximum fire duration,  $\tau$ : as the fire danger index remains  
499 high during most of the dry season, and there is a dominance of grassy PFTs, the  
500 only effects on rate of spread arise from factors associated to grassy PFTs ( $\sigma_{1hr}$ ,  
501 for example) and from changes in wind speed and reduction of the available fuel.  
502 Apart from these two factors,  $a_{Nd}$  is the other parameter controlling the daily

503 burned area, an important contribution in these areas, where human ignitions are  
504 the main source of ignitions and population density weighting is also important.  
505 Simulations (see Fig. 9) confirm the previous points, with Cerrado, Miombo, Sahel  
506 and Mopane showing the importance of  $\sigma_{1hr}$ ,  $\tau$  and  $a_{Nd}$ , with different rank ordering  
507 of the parameters. In general, the very high *TDCC* values suggest that the sites  
508 are homogeneous, and with relatively little inter-annual variation. The Northern  
509 Australian savannas, on the other hand, show an important contribution from soil  
510 moisture through its conversion into live fuel grass moisture content through factor  
511  $\kappa_{\omega}$ . While this factor appears on other sites with a low impact, its importance on  
512 the Northern Australia site is striking. In this site, the phenology of C4 grasses  
513 derived from the MODIS time series has a slow transition from its peak around  
514 March, to its trough around September. This slow decline results in a significant  
515 contribution of live grass to the 1hr fuels up to September. Therefore, parameters  
516 controlling the moisture content of these live grasses, such as  $\kappa_{\omega}$  will have a bearing  
517 on the fuel moisture.

518 In general, the results are quite stable for all regions, with Northern Australia  
519 showing the lowest values of *TDCC*, suggesting a more heterogeneous site.

### 520 3.2.3. Temperate regions

521 [Figure 10 about here.]

522 The sites that belong to the temperate region have a mixture of trees and grasses.  
523 Deciduous trees are quite common, which results in them having an important  
524 contribution to the 1-hr fuels pool through litter accumulation. In these ecosystems,  
525 fuel accumulation can happen over a large number of years due to relative infrequent  
526 fire activity. A typically dry summer is usually long enough to dry fuels, with  
527 ignitions being the major controlling factor in fires. This suggests that in temperate  
528 regions,  $a_{Nd}$  will have a great importance, together with parameters that control  
529 the drying out of fuels, eg  $\alpha$  or  $\sigma_{1hr}$ . Given the conditions conducive to dry fuels,  
530 it is again the duration of the fire, controlled through  $\tau$ , the factor that will have a  
531 very important effect on total burned area.

532 The results (Fig. 10) for Argentina and California are very similar, with  $a_{Nd}$ ,  
533  $\tau$  and  $\sigma_{1hr}$  all being prominent. This is similar to the savanna sites introduced in  
534 Section 2.4.2, and unsurprising, given that these temperate sites are very similar  
535 to the savanna sites (dominant vegetation is grasses, there is a long dry spell, with  
536 moderate to high temperatures).

537 The case of Iberia is more interesting. This region has significant precipitation  
538 during the summer, and moderate temperatures. The factors that control fuel  
539 moisture dynamics are thus of great importance, together with ignition sources. The  
540 lower values of *TDCC* for this region can be ascribed to the higher interannual  
541 meteorological variability controlling fuel moisture.

### 542 3.2.4. Tropical rainforest

543 [Figure 11 about here.]

544 Results for the tropical sites are different. In the Borneo site, the combination  
545 of drivers results in SPITFIRE being unable to simulate fires, unless the moisture  
546 of extinction is low enough to permit fires in typical moist conditions found in  
547 rainforests, with very short lived peaks of  $FDI$  (see Fig. 7(a)). In the Amazonas  
548 site (Fig. 11(a)), there is scope for fire, with the main factors affecting the simulated  
549 annual burned area being those relating to human-caused ignitions, maximum fire  
550 length  $\tau$ . The contribution of the 100-hr fuel class SAV,  $\sigma_{100hr}$ , and the small effect  
551 of  $\alpha$ , as well as the FBD for the tropical evergreen trees suggest that in this site,  
552 rate of spread dynamics also have a direct impact on burned area.

#### 553 4. Discussion

554 A schematic representation of SPITFIRE’s calculation of daily burned area is a  
555 useful starting point to gain insights into the sensitivity analysis results presented in  
556 Section 2.2. Daily burned area is the combination of two terms: ignitions and a mean  
557 fire size. The latter term is a function of rate of spread and fire duration. Ignitions  
558 are controlled mainly by a single parameter,  $a_{Nd}$ , that maps population density into  
559 potential ignitions (lightning ignitions are based on lightning strike climatology).  
560 Rate of spread is a function of the characteristics of fuels present in the simulation  
561 unit, mainly fuel moisture (through a moisture dampening coefficient), fuel structure  
562 (through fuel bulk density and surface-to-area volume) and the amount of fuel  
563 present.

564 Moisture dynamics (calculated by a mapping of the Nesterov Index into a unit-  
565 less moisture scalar) are also controlled by fuel structure through a weighting of the  
566 drying out rate of each fuel class, a parameter related to the ratio of surface-to-area  
567 volume of the different fuel classes. Through the Nesterov Index, fire danger is set  
568 to zero whenever a precipitation event of more than 3mm takes place. However, the  
569 choice of  $\alpha$  and SAVs controls how fast fuels will dry, and hence has an important  
570 knock-on effect on rate of spread calculations by controlling the moisture dampen-  
571 ing coefficient  $\eta$  and the heat of ignition,  $Q_{ig}$ . Broadly speaking, high values of SAV  
572 will result in faster drying rates.

573 In terms of rate of spread, it was shown in Section 3.1.3 that the main fac-  
574 tors affecting its calculation are fuel bulk density,  $\rho_b$  (a parameter specified per  
575 PFT) and SAV. Note that in that part of the study, there is no feedback of SAV  
576 through fuel moisture, as explained above. In general,  $\rho_b$  is indirectly proportional  
577 to rate of spread (although it also plays a role in wind enhancement rate of spread  
578 calculations), while increasing SAV broadly increases rate of spread.

579 The fire danger index also controls fire duration, by scaling the fraction of the  
580 maximum fire duration parameter,  $\tau$ . This has a direct impact on daily burned  
581 area, particularly in situations where the fire danger index is high.

582 The preceding observations suggest that only a handful of factors are likely to  
583 play a role in modelling burned area. The way these factors affect the model output  
584 will be different in different biomes, mostly due to precipitation dynamics. In sites  
585 with large dry spells and high temperatures (typical of savannas and Mediterranean

586 climates), the fire danger index will be unity for most of the dry season (see for  
587 example, Figs. 5(c) or 5(d)), and all fires will last the maximum fire duration. Other  
588 important factors will be those governing rate of spread (the other component of  
589 the mean fire size, and in this case, representative factors are  $\sigma_{1hr}$  and  $\rho_b$ ), as well  
590 as the number of ignitions. However, these parameters will have a limited scope: if  
591 large, long fires burn all the available fuel in a few days at the beginning of the dry  
592 season, increasing potential ignitions will have no effect on total burned area. In  
593 this respect, these parameters have a “buffering” effect by limiting the combustion  
594 of biomass through less ignitions or slower rate of spread. If intermittent rains occur  
595 within the dry season (such as in the Sahel or Mopane sites, Figs. 5(a) and 5(b)),  
596 parameters controlling fuel drying will have an important impact, controlling the  
597 fire danger index during the dry spells between rain events, and hence rate of spread  
598 and fire duration.

599 In the boreal region, low temperatures result in a slower increase of the Nesterov  
600 Index which in turn requires longer dry spells to obtain a fire danger index nearing  
601 unity. This results in these areas having only short spikes of high fire danger index  
602 (e.g. Fig. 4(c)), as these sites experience continental climate regime, with rain  
603 precipitations mainly occurring during the summer period. In addition to that, the  
604 boreal region sites in the taiga region have large amounts of available fuels, with  
605 different fuel classes well-mixed. The combination of short periods conducive to fire  
606 and sufficient available fuel suggests that drying of fuels is a major controlling factor  
607 controlling burned area in the boreal region. Typically, rates of spread in these  
608 regions are moderated by the fuel loads and moisture content of the fuels. This limits  
609 the daily mean fire area calculations, in the same way that low fire danger indices  
610 result in short-lived fires (or in other words, the maximum fire duration is rarely  
611 realised, resulting in little impact of this parameter), an issue already pointed out in  
612 (Thonicke et al., 2010). Ignitions, on the other hand, directly increase on the daily  
613 burned area, and will have a strong effect, but only on those sites where population  
614 density is important (for example, the Canadian site is unpopulated, hence there  
615 can be no modelled human ignitions). The results presented in Section 2.2 confirm  
616 these arguments.

617 The temperate region sites are quite heterogeneous. In this case, the main  
618 climate type is not consistent, in particular in terms of precipitation partitioning  
619 in the summer. While the California site could arguably be labelled as a savanna  
620 site (compare, for example, the fire danger index plots for Northern Australia in  
621 Fig. 5(d) with those of California in Fig. 6(b)), Iberia shows significant precipitation  
622 in the summer (although with fairly large dry spells that allow for fuel drying), with  
623 moderate temperatures, not allowing the fire danger index to increase to unity. This  
624 suggests that parameters that control fuel drying will play an important role in  
625 temperate sites like Iberia or Argentina. In combination with a high fire danger  
626 index during the dry spells, the fire duration is another parameter that can have  
627 a strong effect. This explains the difference between Iberia and Argentina: in the  
628 former,  $\tau$  is only important if the fuel moisture is low, hence the high score of  $\sigma_{1hr}$ .

629 In Argentina, the relatively high temperatures and predominance of fast drying  
630 fuels result in periods of very high FDI, so that  $\tau$  will have an important effect.  
631 In Argentina, there is significant precipitation during the summer, allowing for a  
632 number of short dry spells with fire danger index values close to unity. The analysis  
633 of the California site results is very similar to that of the Sahel site: both sites show  
634 a similar vegetation and climate, and consequently, the results are comparable.

635 SPITFIRE has difficulties producing fires in the rainforest sites. This is due to  
636 the abundance of important rainfall events that results in low values of *FDI*. A  
637 way to produce fires is by lowering the moisture of extinction of the present PFTs,  
638 as fuel moisture is always fairly high due to the continuous rainfall. We observe  
639 that as soon as heterogeneity in PFT distribution is introduced (as is the case in  
640 some grid cells in the Amazonas site that have a significant proportion of grasses),  
641 other factors start playing a role.

## 642 5. Conclusions

643 While the rank order of their importance differs between different biomes, this  
644 study has demonstrated that the following parameters are key influences on simu-  
645 lated burnt area: \*\*\*\*LIST\*\*\*\*.

646 In regions in which ignition sources exist and fuel is abundant but temperatures  
647 are either too low (boreal) or rainfall is too high (tropics), then parameters affect-  
648 ing drying rates of fuels are most important. In regions in which ignition sources  
649 exist and dry fuels exist but fuel buildup is highly variable (tropical savannas and  
650 mediterranean biomes), then parameters associated with the amount of fuel are  
651 most important. Temperate biomes are mixture of both

652 Then you need to tie this back into the introduction eg Flannigan paper describing  
653 what limits fires in boreal zone etc. Lastly I would conclude along the lines of...

654 This study has important implications for the use of SPITFIRE as a model to  
655 predict future fire activity as part of a coupled land-vegetation-atmosphere system  
656 eg QESM (refs). SPITFIRE is demonstrably sensitive to small changes in values of  
657 a small set of parameters affecting sim burnt area. The challenge will be to work out  
658 how to provide better constrained measurements of these parameters using existing  
659 and future EO technologies and field experiments, and then to map these values at  
660 scales relevant to future GCM and earth system modelling.

## 661 Acknowledgements

662 Guido van der Werf is gratefully acknowledged for providing the both the  
663 CASA/GFED code and the GFED 3.1 burned area dataset. The NCEP Reanalysis  
664 data were provided by the NOAA/OAR/ESRL PSD, Boulder, Colorado, USA, from  
665 their Web site at <<http://www.esrl.noaa.gov/psd/>>.

## 666 References

667 Andreae, M. O., Merlet, P., 2001. Emission of trace gases and aerosols from biomass  
668 burning. *Global Biogeochemical Cycles* 15 (4), 955–966.

- 669 Archer, G., Saltelli, A., Sobol, I., 1997. Sensitivity measures, ANOVA-like tech-  
670 niques and the use of bootstrap. *Journal of Statistical Computation and Simula-*  
671 *tion* 58 (2), 99–120.
- 672 Archibald, S., Roy, D., Van Wilgen, B., Scholes, R., 2009. What limits fire?: An  
673 examination of drivers of burnt area in sub-equatorial Africa. *Glob. Chang. Biol*  
674 15, 613–630.
- 675 Arora, V., Boer, G., 2005. Fire as an interactive component of dynamic vegetation  
676 models. *Journal of Geophysical Research* 110 (G2), G02008.
- 677 Bergeron, Y., Gauthier, S., Flannigan, M., Kafka, V., 2004. Fire regimes at the tran-  
678 sition between mixedwood and coniferous boreal forest in northwestern Quebec.  
679 *Ecology* 85 (7), 1916–1932.
- 680 Byram, G., Davis, K., 1959. *Forest fire: control and use*. New York, Editions KP  
681 Davis.
- 682 Campolongo, F., Cariboni, J., Saltelli, A., 2007. An effective screening design for  
683 sensitivity analysis of large models. *Environmental modelling & software* 22 (10),  
684 1509–1518.
- 685 Campolongo, F., Saltelli, A., 1997. Sensitivity analysis of an environmental model:  
686 an application of different analysis methods. *Reliability Engineering & System*  
687 *Safety* 57 (1), 49–69.
- 688 Canadian Forestry Service, 1992. Development and structure of the Canadian for-  
689 est fire behaviour prediction system. Tech. Rep. ST-X-3, Forestry Canada Fire  
690 Danger Group, Ottawa, Ontario, Canada.
- 691 Cochrane, M., Alencar, A., Schulze, M., Souza Jr, C., Nepstad, D., Lefebvre, P.,  
692 Davidson, E., 1999. Positive feedbacks in the fire dynamic of closed canopy trop-  
693 ical forests. *Science* 284 (5421), 1832.
- 694 Cochrane, M. A., 2003. Fire science for rainforests. *Nature* 421 (6926), 913–919.
- 695 Confalonieri, R., Bellocchi, G., Bregaglio, S., Donatelli, M., Acutis, M., 2010.  
696 Comparison of sensitivity analysis techniques: A case study with the rice model  
697 WARM. *Ecological Modelling*.
- 698 Confalonieri, R., Bellocchi, G., Tarantola, S., Acutis, M., Donatelli, M., Genovese,  
699 G., 2009. Sensitivity analysis of the rice model WARM in Europe: Exploring the  
700 effects of different locations, climates and methods of analysis on model sensitivity  
701 to crop parameters. *Environmental Modelling & Software*.
- 702 Flannigan, M., Logan, K., Amiro, B., Skinner, W., Stocks, B., 2005. Future area  
703 burned in Canada. *Climatic change* 72 (1), 1–16.

- 704 Giglio, L., Randerson, J. T., van der Werf, G. R., Kasibhatla, P. S., Collatz, G. J.,  
705 Morton, D. C., DeFries, R. S., 2010. Assessing variability and long-term trends  
706 in burned area by merging multiple satellite fire products. *Biogeosciences* 7 (3),  
707 1171–1186.  
708 URL <http://www.biogeosciences.net/7/1171/2010/>
- 709 Giglio, L., Van Der Werf, G. R., Randerson, J. T., Collatz, G. J., Kasibhatla, P.,  
710 2005. Global estimation of burned area using MODIS active fire observations.  
711 *Atmospheric Chemistry and Physics Discussions* 5 (6), 11091–11141.
- 712 Goldammer, J. G., Furyaev, V. V., 1996. Fire in ecosystems of boreal Eurasia:  
713 ecological impacts and links to the global system. *Fire in ecosystems of Boreal*  
714 *Eurasia* 48, 1–20.
- 715 Goldewijk, K. K., 2005. Three centuries of global population growth: A spatial  
716 referenced population (density) database for 1700–2000. *Population and Envi-*  
717 *ronment* 26, 343–367, 10.1007/s11111-005-3346-7.  
718 URL <http://dx.doi.org/10.1007/s11111-005-3346-7>
- 719 Harris, S., Tapper, N., Packham, D., Orlove, B., Nicholls, N., 2008. The relationship  
720 between the monsoonal summer rain and dry-season fire activity of northern  
721 Australia. *International Journal of Wildland Fire* 17 (5), 674–684.
- 722 Helton, J., Johnson, J., Sallaberry, C., Storlie, C., 2006. Survey of sampling-based  
723 methods for uncertainty and sensitivity analysis. *Reliability Engineering & Sys-*  
724 *tem Safety* 91 (10-11), 1175–1209.
- 725 Kalnay, E., Kanamitsu, M., Kistler, R., Collins, W., Deaven, D., Gandin, L., Iredell,  
726 M., Saha, S., White, G., Woollen, J., et al., 1996. The NCEP/NCAR 40-year  
727 reanalysis project. *Bulletin of the American Meteorological Society* 77 (3), 437–  
728 471.
- 729 Kitzberger, T., Swetnam, T., Veblen, T., 2001. Inter-hemispheric synchrony of forest  
730 fires and the El Niño-Southern Oscillation. *Global Ecology and Biogeography*  
731 10 (3), 315–326.
- 732 Lehsten, V., Tansey, K., Balzter, H., Thonicke, K., Spessa, A., Weber, U., Smith,  
733 B., Arneeth, A., 2008. Estimating carbon emissions from African wildfires. *Bio-*  
734 *geosciences Discussions* 5 (4), 3091–3122.
- 735 Lenihan, J., Daly, C., Bachelet, D., Neilson, R., 1998. Simulating broad-scale fire  
736 severity in a dynamic global vegetation model. *Northwest Science* 72 (4), 91–101.
- 737 Morris, M., 1991. Factorial sampling plans for preliminary computational experi-  
738 ments. *Technometrics* 33 (2), 161–174.
- 739 Peterson, D., Ryan, K., 1986. Modeling postfire conifer mortality for long-range  
740 planning. *Environmental Management* 10 (6), 797–808.

- 741 Potter, C., Randerson, J., Field, C., Matson, P., Vitousek, P., Mooney, H., Klooster,  
742 S., 1993. Terrestrial ecosystem production: a process model based on global satel-  
743 lite and surface data. *Global Biogeochemical Cycles* 7 (4), 811–841.
- 744 Pyne, S., Andrews, P., Laven, R., 1996. Introduction to wildland fire. John Wiley  
745 & Sons Inc.
- 746 Randerson, J. T., Van der Werf, G. R., Collatz, G. J., Giglio, L., Still, C. J.,  
747 Kasibhatla, P., Miller, J. B., White, J. W. C., DeFries, R. S., Kasischke, E. S.,  
748 2005. Fire emissions from C3 and C4 vegetation and their influence on interannual  
749 variability of atmospheric CO<sub>2</sub> and δ<sup>13</sup>C<sub>CO<sub>2</sub></sub>. *Global Biogeochem. Cycles* 19.
- 750 Rothermel, R., 1972. A mathematical model for predicting fire spread in wildland  
751 fuels. Tech. Rep. INT-115, Forest Service, US Department of Agriculture, Ogden,  
752 UT.
- 753 Saltelli, A., 2002. Making best use of model evaluations to compute sensitivity  
754 indices. *Computer Physics Communications* 145 (2), 280–297.
- 755 Saltelli, A., Chan, K., Scott, E., et al., 2004. Sensitivity analysis. Wiley New York.
- 756 Thonicke, K., Spessa, A., Prentice, I. C., Harrison, S. P., Dong, L., Carmona-  
757 Moreno, C., 2010. The influence of vegetation, fire spread and fire behaviour on  
758 biomass burning and trace gas emissions: results from a process-based model.  
759 *Biogeosciences* 7 (6), 1991–2011.  
760 URL <http://www.biogeosciences.net/7/1991/2010/>
- 761 Thonicke, K., Venevsky, S., Sitch, S., Cramer, W., 2001. The role of fire disturbance  
762 for global vegetation dynamics: coupling fire into a Dynamic Global Vegetation  
763 Model. *Global Ecology and Biogeography* 10 (6), 661–677.
- 764 Thorsen, S., Roer, A., van Oijen, M., 2010. Modelling the dynamics of snow cover,  
765 soil frost and surface ice in Norwegian grasslands. *Polar Research* 29 (1), 110–126.
- 766 van der Werf, G., Randerson, J., Collatz, G., Giglio, L., Kasibhatla, P., Arellano Jr,  
767 A., Olsen, S., Kasischke, E., 2004. Continental-scale partitioning of fire emissions  
768 during the 1997 to 2001 El Nino/La Nina period. *Science* 303 (5654), 73.
- 769 van der Werf, G., Randerson, J., Giglio, L., Collatz, G., Mu, M., Kasibhatla, P.,  
770 Morton, D., DeFries, R., Jin, Y., van Leeuwen, T., 2010. Global fire emissions  
771 and the contribution of deforestation, savanna, forest, agricultural, and peat fires  
772 (1997–2009). *Atmos. Chem. Phys. Discuss* 10, 16153–16230.
- 773 van der Werf, G., Randerson, J., Giglio, L., Gobron, N., Dolman, A., 2008. Cli-  
774 mate controls on the variability of fires in the tropics and subtropics. *Global*  
775 *Biogeochemical Cycles* 22 (3).
- 776 Van der Werf, G. R., Randerson, J., Collatz, G., Giglio, L., 2003. Carbon emissions  
777 from fires in tropical and subtropical ecosystems. *Global Change Biology* 9 (4),  
778 547–562.

- 779 Van der Werf, G. R., Randerson, J. T., Giglio, L., Collatz, G. J., Kasibhatla,  
780 P. S., Arellano Jr, A. F., 2006. Interannual variability of global biomass burning  
781 emissions from 1997 to 2004. *Atmospheric Chemistry and Physics Discussions*  
782 6 (2), 3175–3226.
- 783 Van Wilgen, B., Scholes, R., 1997. The vegetation and fire regimes of southern  
784 hemisphere Africa. In: Andreae, M. O., Goldammer, J. G., Lindsay, K. (Eds.),  
785 Fire in southern African savannas. Witwatersand University Press, pp. 27–46.
- 786 Venevsky, S., Thonicke, K., Sitch, S., Cramer, W., 2002. Simulating fire regimes  
787 in human-dominated ecosystems: Iberian Peninsula case study. *Global Change*  
788 *Biology* 8 (10), 984–998.
- 789 Whelan, R. J., 1995. The ecology of fire. Cambridge Univ Press.

790 **List of Figures**

791	1	A diagram showing the main processes that influence the calculation	
792		of daily burned area in SPITFIRE. . . . .	24
793	2	A cartoon example of typical output from the Morris methodology.	
794		This fictitious example has five factors, <i>A</i> , <i>B</i> , <i>C</i> , <i>D</i> and <i>E</i> . . . . .	25
795	3	Spatial distribution of test sites . . . . .	26
796	4	Fire Danger index. Boreal region sites . . . . .	27
797	5	Fire Danger Index. Savannah sites . . . . .	28
798	6	Fire Danger Index. Temperate region sites . . . . .	29
799	7	Fire Danger Index. Tropical region sites . . . . .	30
800	8	Results of sensitivity analysis. Boreal region sites . . . . .	31
801	9	Results of sensitivity analysis. Savannah sites . . . . .	32
802	10	Results of sensitivity analysis. Temperate region sites . . . . .	33
803	11	Sensitivity analysis of the (a) Amazonas and (b) Borneo sites. . . . .	34

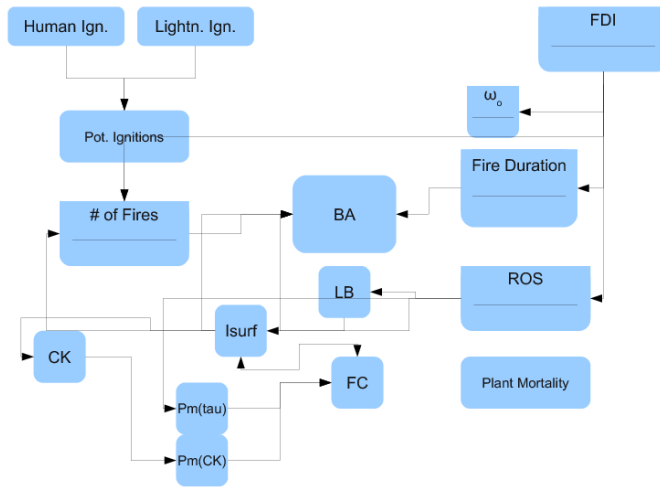


**Figure 1:** A diagram showing the main processes that influence the calculation of daily burned area in SPITFIRE.

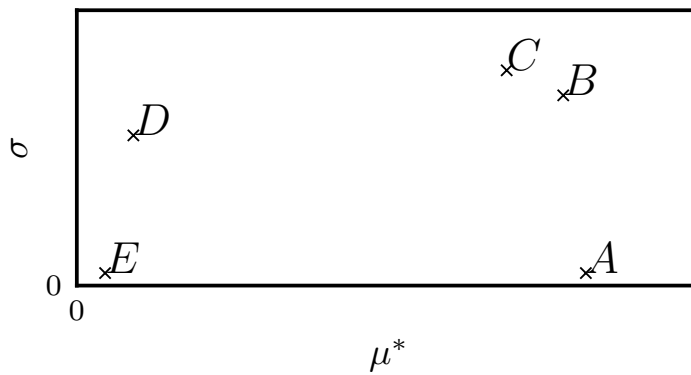


**Figure 2:** A cartoon example of typical output from the Morris methodology. This fictitious example has five factors,  $A$ ,  $B$ ,  $C$ ,  $D$  and  $E$ .

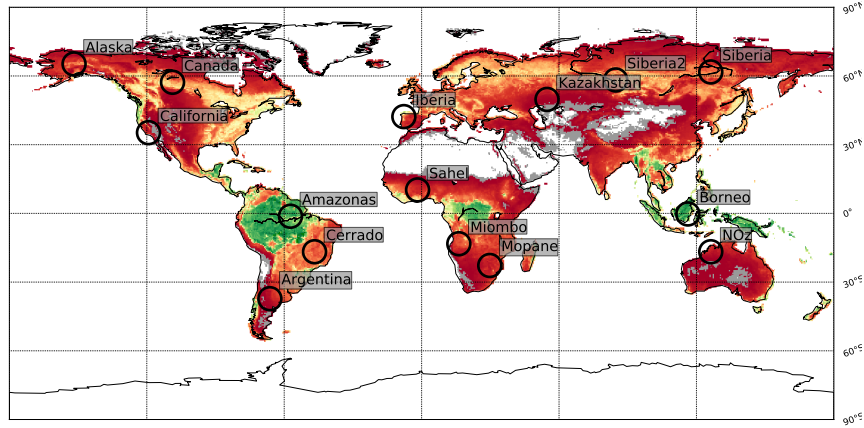
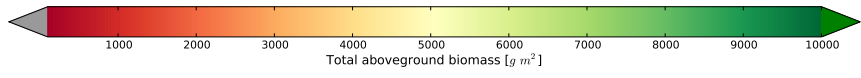
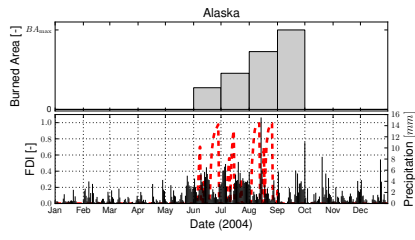
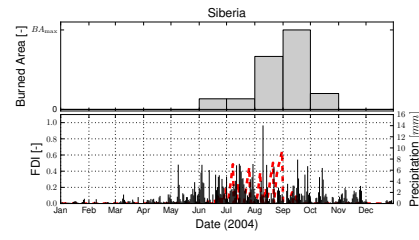


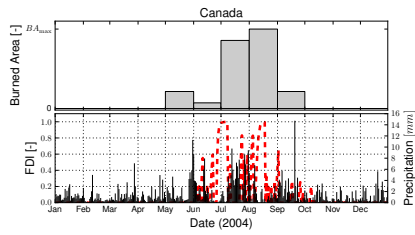
**Figure 3:** Spatial distribution of test sites



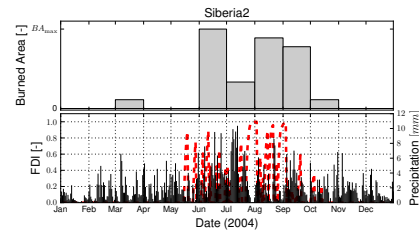
(a) Alaska



(b) Siberia



(c) Canada



(d) Siberia 2

**Figure 4:** Distribution of monthly burned area according to GFED3 (Giglio et al., 2010) (top panels), and temporal evolution of the fire danger index (FDI) for the boreal region sites in 2004: (a) Alaska , (b) Siberia, (c) Canada and (d) Siberia2.

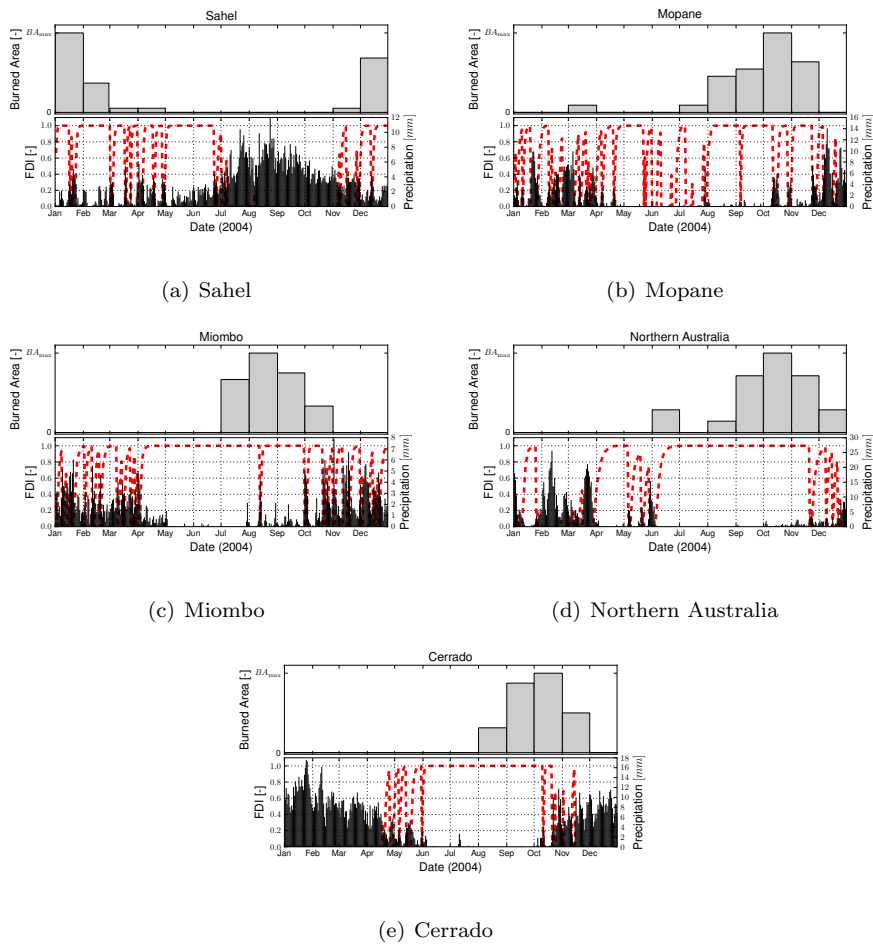
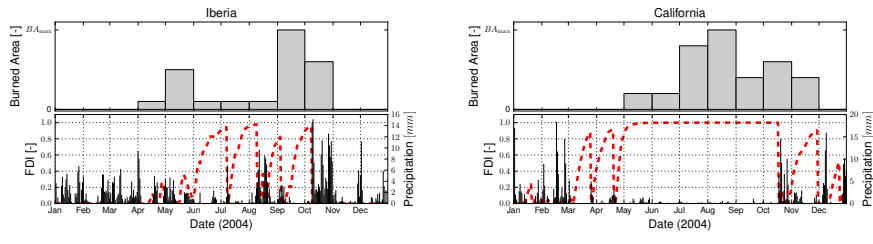
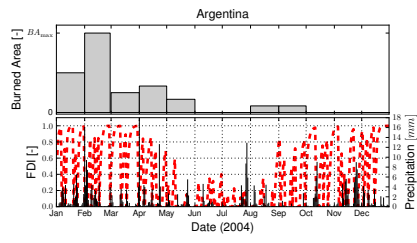


**Figure 5:** Distribution of monthly burned area according to GFED3 (Giglio et al., 2010) (top panels), and temporal evolution of the fire danger index (FDI) for the savanna sites in 2004: (a) Sahel, (b) Mopane, (c) Miombo, (d) Northern Australia and (e) Cerrado.



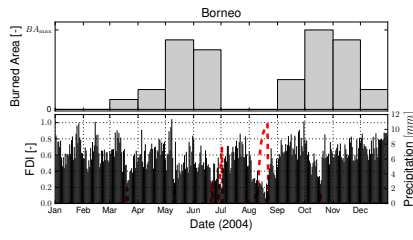
(a) Iberia

(b) California

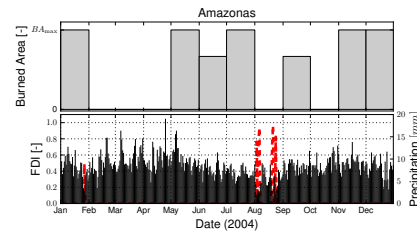


(c) Argentina

**Figure 6:** Distribution of monthly burned area according to GFED3 (Giglio et al., 2010) (top panels), and temporal evolution of the fire danger index (FDI) for the temperate region sites in 2004: (a) Iberia, (b) California and (c) Argentina.



(a) Borneo



(b) Amazonas

**Figure 7:** Distribution of monthly burned area according to GFED3 (Giglio et al., 2010) (top panels), and temporal evolution of the fire danger index (FDI) for the tropical region sites in 2004: (a) Borneo and (b) Amazonas.

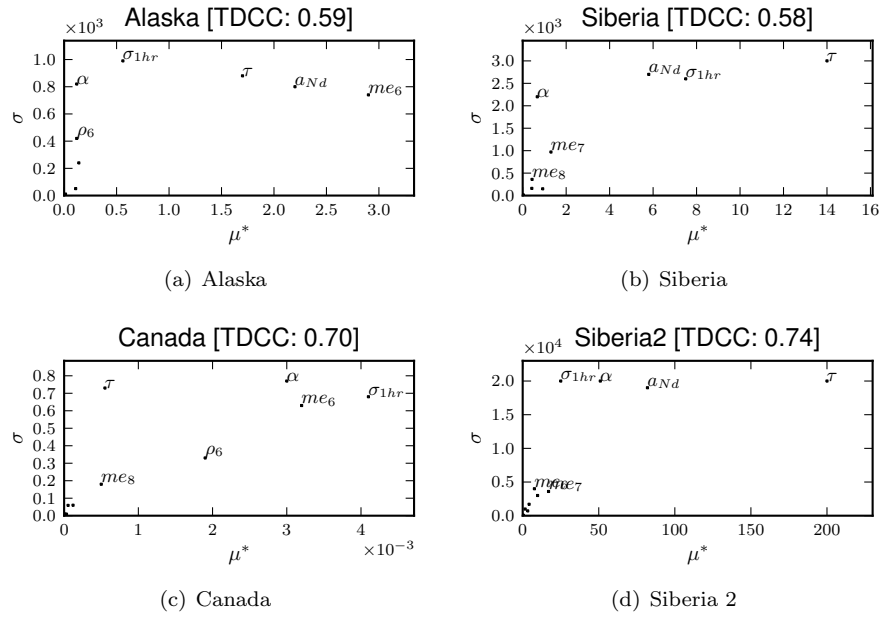


**Figure 8:** Sensitivity analysis results for the boreal region sites: (a) Alaska, (b) Siberia, (c) Canada and (d) Siberia 2.

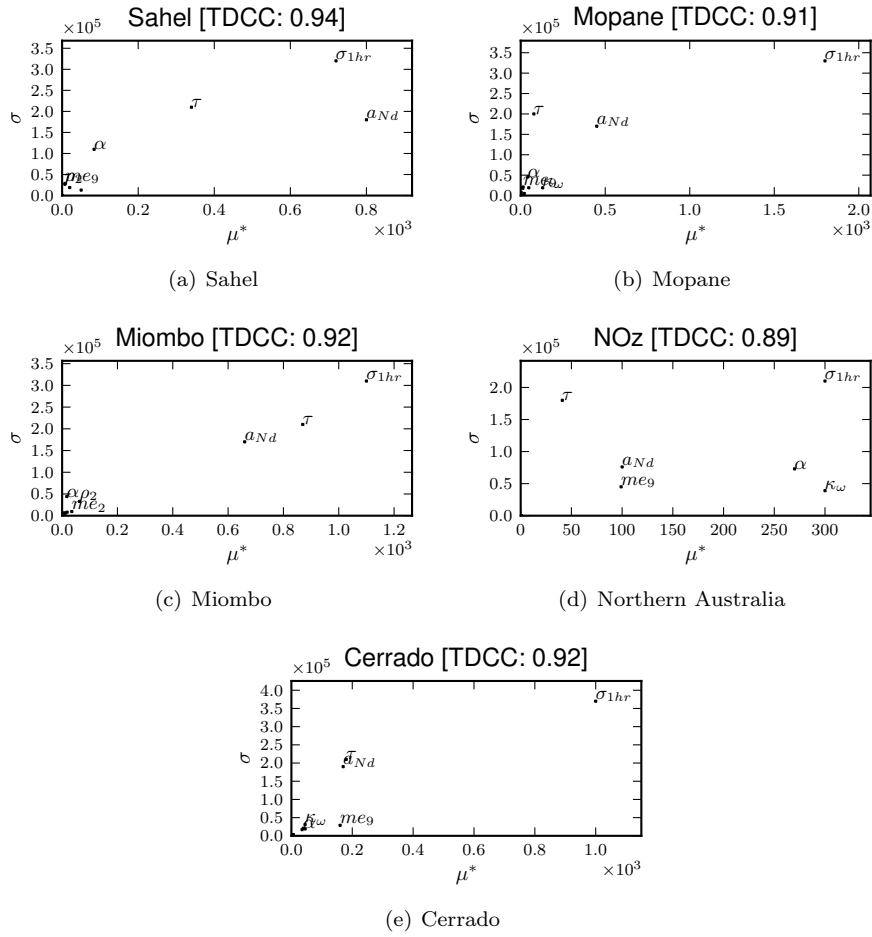


**Figure 9:** Sensitivity analysis results for the savanna sites: (a) Sahel, (b) Mopane, (c) Miombo, (d) Northern Australia and (e) Cerrado.

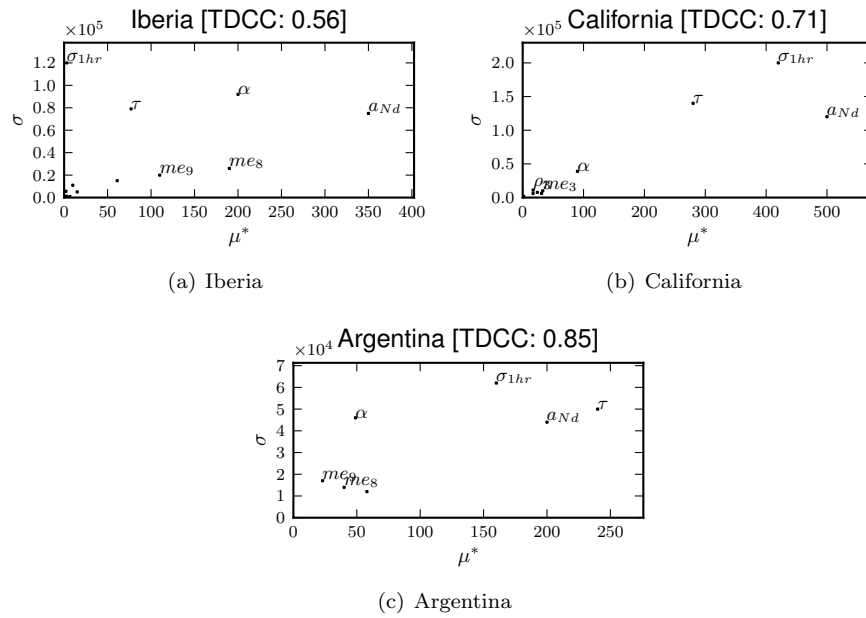
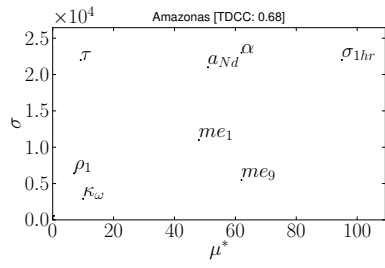
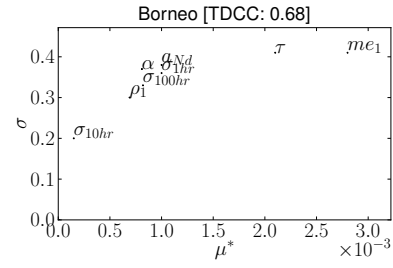


**Figure 10:** Sensitivity analysis results for the temperate region sites: (a) Iberia, (b) California and (c) Argentina.



(a) Amazonas



(b) Borneo

**Figure 11:** Sensitivity analysis of the (a) Amazonas and (b) Borneo sites.

804 **List of Tables**

805	1	Description of sites . . . . .	36
806	2	Sensitivity analysis of Rate of Spread according to Rothermel's equations. . . . .	37
807			
808	3	Sensitivity analysis of Rate of Spread according to Rothermel's equations for dry fuels. . . . .	38
809			
810	4	Parameters included in the sensitivity analysis exercise, with the symbol used in the text, the range of values used, the default values used in (Thonicke et al., 2010) and the units. . . . .	39
811			
812			

**Table 1:** Description of sites

Site	Dominant PFTs <sup>a</sup>	1hr Fuel <sup>b</sup>	10hr Fuel <sup>b</sup>	100hr Fuels <sup>b</sup>
Canada	BoNLEvgn	594.77	617.32	1030.54
Alaska	BoNLEvgn	602.61	257.15	512.83
Siberia	BoSgn	243.84	473.46	1016.93
Siberia2	BoNLEvgn BoSgn	709.61	640.70	1233.38
Miombo	TrBLRgn C3 C4	787.11	194.00	454.50
Sahel	C4	634.77	34.11	30.34
NOz	C4	410.49	0.00	0.00
Mopane	C4	414.24	51.48	87.04
Cerrado	C4	1044.12	110.87	280.65
California	C3 C4	240.26	45.13	140.52
Iberia	C3 TeNLEvgn TeBLSgn C4	862.82	393.92	1095.64
Argentina	C4	66.08	0.00	0.00
Borneo	TrBLEvgn	2162.08	1149.24	2740.49
Amazonas	TrBLEvgn	2669.50	1400.41	3436.49

<sup>a</sup> PFTs are TrBLEvgn: tropical broadleaved evergreen trees, TrBLRgn: tropical broadleaved raingreen trees, TeNLEvgn: temperate needleleaved evergreen trees, TeBLEvgn: temperate broadleaved evergreen trees, TeBLSgn: temperate broadleaved summergreen trees, BoNLEvgn: boreal needleleaved evergreen trees, BoSgn: boreal summergreen trees, C3: C3 grasses, C4: C4 grasses

<sup>b</sup> Maximum values for 2004 simulated using GFED/CASA.

<b>Factor</b>	<b>Minimum value</b>	<b>Maximum value</b>	$S_i$	$S_{T_i}$
Fuel bulk density	0.1	40	0.005	0.92
Surface-area volume	0.1	200	0.001	0.59
Fuel moisture content	0	1	0.01	0.95
Wind speed	1	500	0.001	0.13
Particle Density	410	614	$\sim 0$	0.002
Heat content	144000	21600	$\sim 0$	0.026
Total mineral content	0%	10%	$\sim 0$	0.006

**Table 2:** Sensitivity analysis of Rate of Spread according to Rothermel's equations.

<b>Factor</b>	<b>Minimum value</b>	<b>Maximum value</b>	$S_i$	$S_{T_i}$
Fuel bulk density	0.1	40	0.1	0.95
Surface-area volume	0.1	200	0.1	0.48
Fuel moisture content	0	0.1	$\sim 0$	0.06
Wind speed	1	500	0.001	0.46
Particle Density	410	614	$\sim 0$	0.003
Heat content	144000	21600	$\sim 0$	0.016
Total mineral content	0%	10%	$\sim 0$	0.01

**Table 3:** Sensitivity analysis of Rate of Spread according to Rothermel's equations for dry fuels.

Parameter	Symbol	Min val.	Max. val.	Def. val.	Units
SAV 1hr fuels	$\sigma_{1hr}$	5	300	66	$cm^{-1}$
SAV 10hr fuels	$\sigma_{10hr}$	0.49	1.47	3.58	$cm^{-1}$
SAV 100hr fuels	$\sigma_{100hr}$	1.8	5.4	0.98	$cm^{-1}$
Moisture constant 1hr	$\alpha_{1hr}$	5E-4	4E-3	1E-3	$^{\circ}C^2$
Moisture extinction 1	$m_{e,1}$	0.1	0.3	0.2	–
Moisture extinction 2	$m_{e,2}$	0.1	0.5	0.3	–
Moisture extinction 3	$m_{e,3}$	0.1	0.5	0.3	–
Moisture extinction 4	$m_{e,4}$	0.1	0.5	0.3	–
Moisture extinction 5	$m_{e,5}$	0.1	0.5	0.3	–
Moisture extinction 6	$m_{e,6}$	0.1	0.5	0.35	–
Moisture extinction 7	$m_{e,7}$	0.1	0.5	0.35	–
Moisture extinction 8	$m_{e,8}$	0.1	0.5	0.2	–
Moisture extinction 9	$m_{e,9}$	0.1	0.5	0.2	–
Fire Duration factor	$\tau$	0.01	5	10.9	–
Anthr. ign. factor	$a_{Nd}$	0.05	15	0.3	UNITS
Fuel Bulk Density 1	$\rho_1$	10	25	14	$kgm^{-3}$
Fuel Bulk Density 2	$\rho_2$	10	25	12	$kgm^{-3}$
Fuel Bulk Density 3	$\rho_3$	16	31	23	$kgm^{-3}$
Fuel Bulk Density 4	$\rho_4$	10	16	28	$kgm^{-3}$
Fuel Bulk Density 5	$\rho_5$	13	22	22	$kgm^{-3}$
Fuel Bulk Density 6	$\rho_6$	18	30	18	$kgm^{-3}$
Fuel Bulk Density 7	$\rho_7$	16	22	16	$kgm^{-3}$
Fuel Bulk Density 8	$\rho_8$	1	2	4	$kgm^{-3}$
Fuel Bulk Density 9	$\rho_9$	1	2	2	$kgm^{-3}$

**Table 4:** Parameters included in the sensitivity analysis exercise, with the symbol used in the text, the range of values used, the default values used in (Thonicke et al., 2010) and the units.